ISSN 1392-1207. MECHANIKA. Vol. 29, No. 4, 2023: 324–333

Lubrication Analysis of Hydrodynamic-Static Hybrid Bearing with Deep-Shallow Chambers Considering Thermal Conduction

Qianwen HUANG*, Zeyu ZHAO, Huaiguang LIU*****
**Hubei Key Laboratory of Mechanical Transmission and Manufacturing Engineering, School of Machinery and Automation, Wuhan University of Science and Technology, Wuhan, 430081, China, E-mail: qwhuang@wust.edu.cn*
***School of Machinery and Automation, Wuhan University of Science and Technology, Wuhan, 430081, China, E-mail: 574450367@qq.com*
****Hubei Key Laboratory of Mechanical Transmission and Manufacturing Engineering, School of Machinery and Automation, Wuhan University of Science and Technology, Wuhan, 430081, China, E-mail: liuhuaiguang@wust.edu.cn*
https://doi.org/10.5755/j02.mech.33196

1. Introduction

The shaft-bearing system is one of the most important friction conjunctions applied in the power transmission systems of machines. With the advantages of great capacity of load carrying and minor sensitivity of variable loads, the deep-shallow journal bearing is applied in various mechanical transmission systems [1]. In order to diminish friction and reduce wear of the contact surface between the rotational shaft and journal bearing, the fluid pressure generated by the motion of oil film will separate the contact pair completely [2, 3]. Therefore, the hydrodynamic lubrication of journal bearing is greatly related to the operational reliability and working efficiency with the high demand of load carrying capacity [4]. The lubrication behaviour of journal bearing is thus great significant, especially in forming dynamic pressure properties of oil film [5].

The hydrodynamic bearing operated with high rotational speed and extreme load, which no doubt causes larger temperature variation [6]. This excessive temperature is more severe with lower rotational speed because of inadequate film pressure [7, 8]. Part of the heat generated by the shear of lubricated film transfers to the bearing components and the oil film [9]. The fluid pressure will increase and the film thickness will decrease with the temperature increase [10]. Therefore, the thermo-hydrodynamic (THD) lubrication of the journal bearing is significantly affected by the thermal conduction [11, 12]. Therefore, it is important to consider the temperature variation of the oil film.

By neglecting the inertia terms in the more general Navier-Stokes theory, the Reynolds equation [13], which takes account of viscous effects, is widely applied in the calculation of THD lubrication with low rotational speed. With reasonable application of Reynolds equation involved in the theoretical model, the THD lubrication of the bearing was gradually elaborated. U. Singh et al. [14] found the temperature of the oil film raised because of the frictional heat. The effect of shaft speed, supply pressure and bearing structural size were discussed. L. Roy et al. [15] demonstrated that the load capacity, end flow rate, fluid pressure and film temperature increase with rotational speed of the shaft. X. Zhang et al. [16] calculated the pressure distribution, load capacity and friction performance on the basis of CFD simulation, with a comparison of results for geometry optimization. Y. Wang et al. [17] indicated that the friction coefficient increases significantly with working temperature, and it decreases distinctly with rotational speed. Y. Zhang et al. [18] analysed the characteristics of temperature variation, and the temperature rise curves with variable rotating speed and inlet flow velocity were obtained.

Meanwhile, with gradual maturity of theoretical basis, related numerical calculation was developed along with the improvement of computer capability. A variety of methods have been applied to calculate the THD lubrication of deep-shallow journal bearing. For example, the finite difference method (FDM) [19], computational fluid dynamic (CFD) [20], finite element method (FEM) [21], CFD coupled with FEM method [9], and fluid-structure interaction (FSI) technique [22]. Moreover, the experimental investigation [17, 18] was carried out with high precision equipment and sensors. These researches provide possible theories to explain the mechanism and feasible methodology to calculate the behaviour of THD lubrication.

However, the applicability of published works regarding the lubrication behaviour of journal bearing with deep-shallow chambers considering thermal conduction is limited. The analytical method includes complex nonlinear equations to be solved, and the numerical simulation requires large grid to be computed. Moreover, it has been demonstrated that multiple impact factors have a significant influence on the THD lubrication of the bearing. The load capacity is much related to the distribution of oil film [23], the variation of film thickness, pressure and temperature is caused by the shaft speed [24], and the interaction between fluid pressure and temperature is produced [25]. Therefore, only limited investigations are flexible enough to deal with the THD lubrication considering these impact factors simultaneously.

In view of this, a numerical model regarding the THD lubrication of the hydrodynamic-static hybrid bearing with deep-shallow chambers is proposed. The model is verified by a comparison with experimental tests and theoretical analysis in published literature. The lubrication behaviour includes fluid pressure, load capacity, bearing stiffness and flow rate is numerically calculated. The impact factor includes film thickness, working temperature and eccentricity ratio is investigated. Furthermore, the temperature variation of thermal conduction is analysed in detail. The lubrication performance with constant and variable temperatures is also compared to investigate the influence of thermal conduction. On this basis, a practicable calculation of the THD lubrication of the bearing with multiple impact factors is realized.

2. Theoretical basis

2.1. Lubrication behaviour

The Fig. 1 shows the cross-sectional diagram and pressure distribution of a lubricated journal bearing, which consists of orifice restrictors, deep-shallow chambers and return chutes. The x-axis and y-axis represent the horizontal and vertical direction, respectively. The structural parameter φ_{11} is the angle from the head of the deep chamber to the negative direction of the y-axis, φ_{12} is the angle from the end of the shallow chamber to the negative direction of the y-axis, φ_b is the circumferential angle of the sealing oil edge and φ_c is the angle of the deep chamber. The eccentricity is e, the rotational speed of shaft is ω, the film thickness is h and the supplied fluid pressure is p_s.

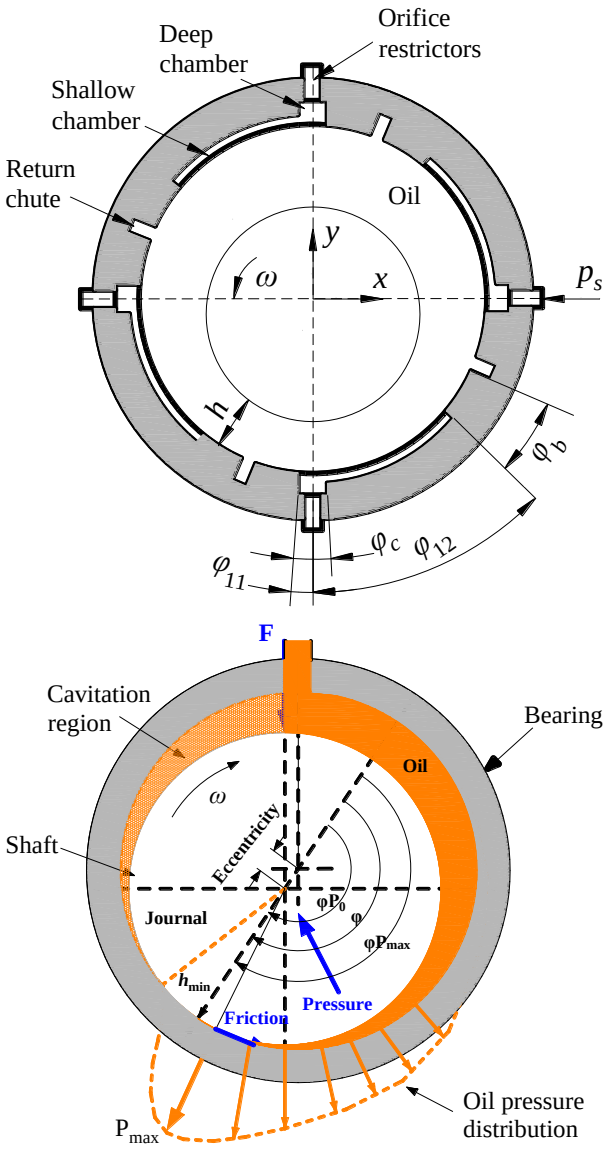

Fig. 1 Structural diagram and pressure distribution of lubricated journal bearing [26]

The oil film enters the deep chamber through an orifice throttle due to supplied pressure. It flows to the shallow chamber after the migration of the shaft journal and the secondary throttling between deep-shallow chambers. The dynamic pressure is thus formed at the end of the shallow chamber whose amplitude is greater than that of the deep chamber. Finally, the oil film enters the return chutes by sealing the oil edge. The Reynolds equation for lubrication behavior can be expressed as [27]:

$$\frac{\partial}{\partial r}\left(\frac{rh^3}{\mu}\frac{\partial p}{\partial r}\right)+\frac{1}{r}\frac{\partial}{\partial \theta}\left(\frac{h^3}{\mu}\frac{\partial p}{\partial \theta}\right)=6r\omega\frac{\partial h}{\partial \theta}, \tag{1}$$

where: h is the film thickness; p is the fluid pressure; μ is the lubricant viscosity of the oil film; ω is the rotational speed of the shaft; θ and r represent the circumferential and radial direction.

The lubricant viscosity of the oil film is defined as:

$$\mu=v\rho, \tag{2}$$

where, the kinematic viscosity v is the flow resistance under the action of gravity; ρ is density of the oil film.

Assuming that the film thickness is much smaller than that of the bearing radius, the film thickness of any circumferential angle can be expressed as:

$$h=c(1-\varepsilon cos\theta), \tag{3}$$

where: c is the radial clearance; ε is the eccentricity ratio which can be given as:

$$\varepsilon=\frac{e}{c}, \tag{4}$$

where, the eccentricity e is the distance between the shaft center and the sleeve at half length of the bearing.

The load capacity of the bearing can be obtained through the sum of each chamber, which is calculated by an integration of the fluid pressure:

$$F=\int_{\varphi_{11}-\varphi_b/2}^{\varphi_{11}+\varphi_b/2} p(L-l)Rcos\theta d\theta, \tag{5}$$

where: L and R are the length and radius of the bearing. The length of the oil chamber is represented by l.

Therefore, the bearing stiffness can be calculated by the derivative of load capacity to film thickness, which is expressed as:

$$k=\frac{\partial F}{\partial h}=\frac{\partial F}{h_0 cos\theta\cdot\partial\varepsilon}, \tag{6}$$

where the bearing stiffness in vertical direction can be obtained with the condition of $\theta=0$.

2.2. Thermal conduction

The thermal conduction of the oil film has a great influence on the lubrication behavior, especially with higher rotational speed [28]. With the flow rate on the journal bearing and friction force on the contact surface, the temperature variation can be given with the following empirical formula:

$$\Delta T=\frac{N_p+N_f}{JC_0\rho\Sigma Q}, \tag{7}$$

where: N_p and N_f are the power of flow rate and friction force, respectively. The J is the mechanical equivalent of heat and

C_0 is the specific heat capacity. The ΣQ is the total flow of the bearing with Q is that of a single chamber, which can be calculated through flow rate multiplied by the area.

The effective area of single chamber A_e can be given as:

$$A_e = (L-l)R\left(sin\left(\varphi_{12} + \frac{\varphi_c}{2} \right) - sin\theta_1 \left(\varphi_b - \frac{\varphi_c}{2} \right) \right). \quad (8)$$

The effective area of the bearing is the total sum of each chamber. Therefore, the power of the bearing N_p can be calculated by the pressure and total flow, which is expressed as:

$$N_p = p\Sigma Q. \quad (9)$$

The consumed power of friction is induced by the velocity variation of the shaft under the viscous resistance of the oil pad. Hence, the power of the friction force can be expressed as:

$$N_f = \Sigma F_f v_s, \quad (10)$$

where: F_f is the friction force; v_s is the velocity of the shaft which can be defined as:

$$v_s = R\omega. \quad (11)$$

According to the law of Newton's inner friction, the viscous resistance that an oil chamber produces as the shear of oil film can be given by:

$$F_f = \mu A_s \frac{v_s}{h} + \mu A_r \frac{v_s}{h + \Delta h}, \quad (12)$$

where: Δh is the step length that is defined as 2.5 mm; A_s is the area of the sealing oil edge around the chambers, which can be given by:

$$A_s = LR(\varphi_{12} - \varphi_c + 2\varphi_b) - A_r, \quad (13)$$

where: A_r is the area of the deep and shallow chambers, which can be calculated by:

$$A_r = (L-2l)R(\varphi_{12} - \varphi_c). \quad (14)$$

The following assumptions are made: 1. The oil film flows with a laminar steady state; 2. The pressure distribution in Fig. 1 is simplified as piecewise linear pressure; 3. The axis offset of vertical downward is supposed to be zero (misalignment angle is 0°); 4. The oil film is in isothermal condition and the viscosity remains unchanged as small variation in temperature; 5. All the heat is absorbed by the lubricating oil and taken away by the end leakage.

3. Model validation

In order to validate the proposed model, a comparison of numerical results is conducted with published literature. The model parameters of numerical calculation are defined to be consistent with the study case given by S. Meng et al. [29]. Specific data of the supply pressure is defined as 2.0, 2.5 and 3.0 MPa with a rotational speed of 0, 2000 to 4000 r/min, respectively. The results of temperature variation are selected for the model validation. Therefore, a comparison between the experimental test, theoretical analysis and proposed model in this work is listed in Table 1.

The results indicate that the temperature variation calculated in this paper is much consistent with experimental test and theoretical analysis in published literature over a range of supply pressure and rotational speed.

Table 1

Difference of temperature variation with experimental test and theoretical analysis [29]

Pressure p_s, MPa	Rotation ω, rpm	Tests ΔT, ℃	Theory ΔT, ℃	Proposed ΔT, ℃	Diff. with Test, %	Diff. with Theory, %
2.0	2000	4.8	4.11	4.27	11.04	3.89
	4000	12.8	11.97	11.87	7.26	0.83
2.5	2000	4.5	4.03	4.22	6.22	4.71
	4000	11.8	11.16	11.21	5.00	0.45
3.0	2000	4.4	4.04	4.21	4.31	4.21
	4000	11.5	10.6	10.67	7.21	0.66

The largest difference is 11.04 %, which represents the comparison between test and this work with the supply pressure is 2.0 MPa and rotational speed is 2000 r/min. The difference may be caused by certain differences between the actual value and the defined value. And the experiment, including operation status, acquisition method and structural characteristics will lead to a deviation from the numerical calculation. The confidence level of the comparison is much high and can be accepted for the model validation.

4. Result analysis

In order to investigate the lubrication behavior of the bearing, the numerical calculation is conducted on the basis of theoretical Eqs. (1 – 6), which are solved by the centered finite difference method. The values of parameters applied in the proposed model are summarized in Table 2.

The centered finite difference method is applied to solve the Reynolds equation with Matlab code. Appling a supply pressure to calculate the pressure distribution of the oil film and the load capacity of the bearing. Determining the criteria of the number of iterations is:

$$\frac{\sum_{i=2}^{m}\sum_{j=2}^{n}\left|\overline{p}_{i,j}^{(k)} - \overline{p}_{i,j}^{(k\text{-}1)}\right|}{\sum_{i=2}^{m}\sum_{j=2}^{n}\left|\overline{p}_{i,j}^{(k)}\right|} < \xi, \quad (15)$$

where: k is the number of iterations, m and n are the number of grids in the circumferential and axial directions, which are defined as 100 steps, the value of ξ is defined as $\xi = 1.0\times10^{-4}$.

As it is noticed that multiple impact factors will affect the lubrication behavior, and the proposed method is

validated to be suitable for the numerical calculation. In order to investigate the influence, two specific cases with various film thicknesses and working temperatures are defined. Besides the eccentricity ratio is also considered in each case study for comparison. The lubrication behavior includes fluid pressure, load capacity, bearing stiffness and flow rate are thus analyzed to determine the operational state of the bearing. It should be pointed out that as the value of each parameter changes, others remain the initial values in Table 2.

Table 2

Model parameters in numerical calculation

Parameters	Values
Journal radius, m	0.07
Bearing length, m	0.25
Length of oil chamber, m	0.023
Radial clearance, mm	0.05
Angle of shallow chamber, °	42
Angle of sealing oil edge, °	3.0
Angle of deep chamber, °	1.5
Film density, Kg/m^3	860
Kinematic viscosity, mm^2/s	10
Eccentricity, mm	0.01
Supply pressure, MPa	3.0
Temperature, °C	30
Mechanical equivalent of heat, Kg·m/Kcal	427
Specific heat capacity, cal/Kg·°C	0.5
Total flow rate, cm^3/s	833
Rotational speed, r/min	100

4.1. Effect of film thickness on lubrication

The results in Fig. 2 show the fluid pressure, load capacity, bearing stiffness and flow rate of the journal bearing with the film thickness ranges from 0.01 to 0.05 mm, respectively. The fluid pressure in Fig. 2, a decreases with increasing film thickness and trends to be stable at about 0.05 mm. The fluid pressure-film thickness curve in Fig. 2, a seems to be an inversely proportional function. The decay from more than 100 to about 2 MPa, which is about two orders of magnitude.

The effect of film thickness on load capacity and bearing stiffness is illustrated in Figs. 2, b and c, which seems much similar to the results in Fig. 2, a. It can be observed to be decreased with an order of magnitude as the film thickness increases. And both the result tends to be stable with the film thickness at the position of about 0.05 mm. It can be noticed that the effect of film thickness on the load capacity is much more sensitive than that of the fluid pressure and bearing stiffness. That is because the variation in Fig. 2, b is more obvious, while the partial enlargement in Figs. 2, a and c are nearly unchanged with increasing film thickness. The result in Fig. 2, d indicates that the flow rate of the fluid increased with the film thickness ranges from 0.01 to 0.05 mm. The variation trends of flow rate to be linear relationship, comparing between the results of Figs. 2, a to c.

Moreover, the lubrication behavior of the bearing is observed to be increased with the eccentricity ratio ranges from 0.01 to 0.05. That means the eccentricity ratio will enlarge the lubrication performance of the bearing. The variation of load capacity with different eccentricity ratio is observed to be much larger, while other appear to be unchanged. It means that the load capacity is more sensitive to the eccentricity ratio.

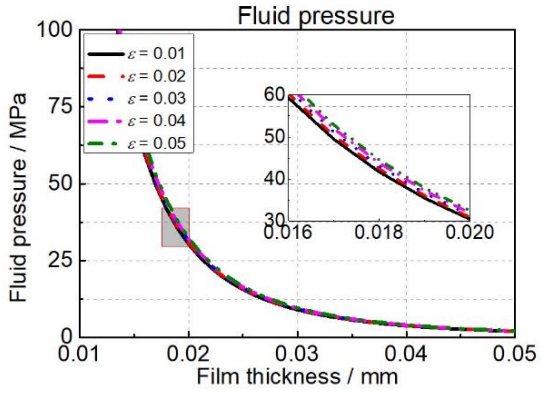

a

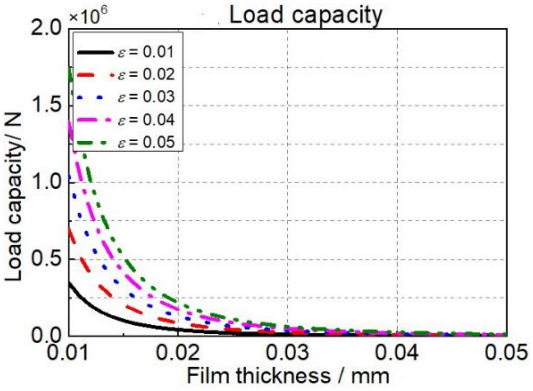

b

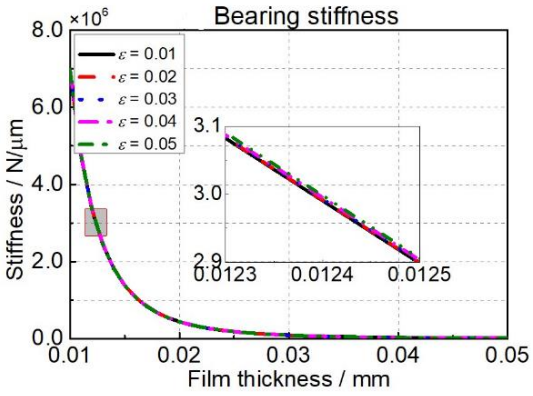

c

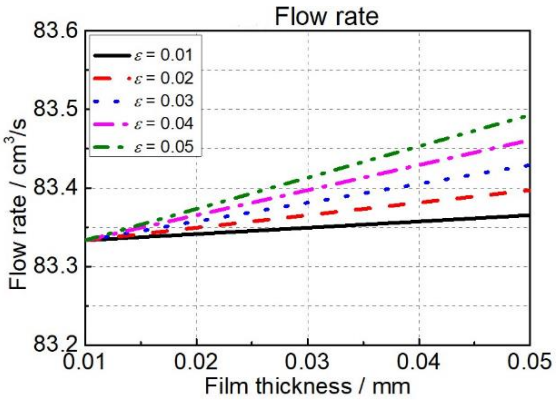

d

Fig. 2 The lubrication behavior of various film thickness: a) Fluid pressure; b) load capacity; c) bearing stiffness; d) flow rate

4.2. Effect of working temperature on lubrication

The results in Fig. 3 are the fluid pressure, load capacity, bearing stiffness and flow rate with the working temperature ranges from 0 to 80°C, respectively. Fig. 3, a shows the fluid pressure decreases significantly with the temperature ranges from 0 to 60°C, and then decreases slowly as the temperature increases from 60 to 80°C. The decay can also be noticed in the variation of load capacity and bearing stiffness, shown in Fig. 3, b and c. Moreover, it can be noticed that these variations in lower temperature are more pronounced than that of the higher temperature. While the flow rate in Fig. 3, d changes slightly with the temperature increases from 0 to 80°C.

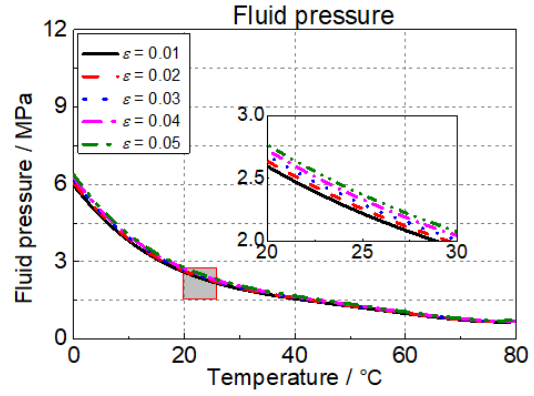

a

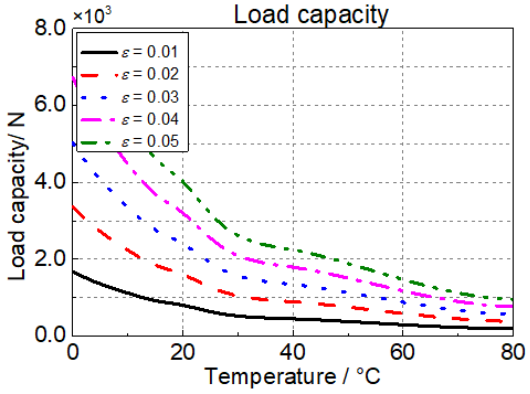

b

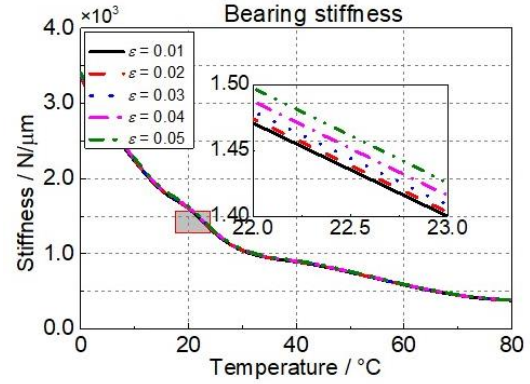

c

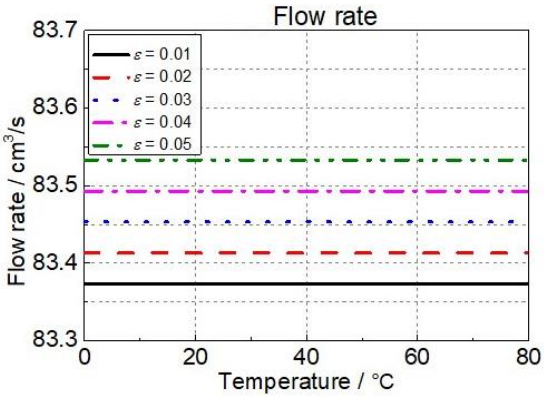

d

Fig. 3 The lubrication behavior with various temperature: a) fluid pressure; b) load capacity; c) bearing stiffness; d) flow rate

Comparing the variation with different eccentricity ratio, the THD lubrication is noticed to be increased with increasing eccentricity ratio. The variation of load capacity in Fig. 3, b is observed to be much larger. While the variation of fluid pressure in Fig. 3, a, bearing stiffness in Fig. 3, c and flow rate in Fig. 3, d are noticed to be much slight. That means the load capacity is the most sensitive with the effect of the eccentricity ratio.

5. Thermal conduction

In general, it can be concluded that the lubrication behavior of the bearing is closely affected by the film thickness, rotational speed, working temperature and eccentricity ratio. While as it is mentioned in the Eq. (7) of the theoretical basis that the working temperature of the oil film is not constant. The thermal conduction will be produced with the action of friction power and flow power, leading to a variable temperature. In practice, the journal bearing experiences substantial thermal effects during operation so that the working temperature is usually considerably higher than the supplied. Therefore, it is crucial to take the thermal conduction into account when analyzing the lubrication performance of the bearing.

In order to investigate the temperature variation caused by thermal conduction, the Eqs (7)–(14) are considered in the lubrication analysis. The temperature variation with various eccentricity ratios, film thickness and rotational speed is thus analyzed. The eccentricity ratio is defined as 0.01, 0.02, 0.03, 0.04 and 0.05, the film thickness ranges from 0.02 to 0.04 mm with an increment of 0.005 mm, the rotational speed is set as 50 to 150 r/min with a step of 25 r/min. During the calculation, the criteria of the number of iterations for the temperature is determined as:

$$\frac{\sum_{i=2}^{m}\sum_{j=2}^{n}\left|\overline{T}_{i,j}^{(k)}-\overline{T}_{i,j}^{(k-1)}\right|}{\sum_{i=2}^{m}\sum_{j=2}^{n}\left|\overline{T}_{i,j}^{(k)}\right|}<\xi, \tag{16}$$

where, the values of parameters k, m, n and ξ keep the same with that of Eq. (15).

The results in Fig. 4 shows the temperature variation of thermal conduction with various eccentricity ratio and rotational speed. It can be seen in Fig. 4, a that the temperature increases slightly with the eccentricity ratio increases from 0.01 to 0.05. This phenomenon exists for every speed condition. And for a particular speed, the temperature is noticed to be enlarged with the increasing rotational speed. The results in Fig. 4, b show the temperature variation with film thickness from 0.02 to 0.04 mm is much more obvious. It shows a rapid decrease with increasing film

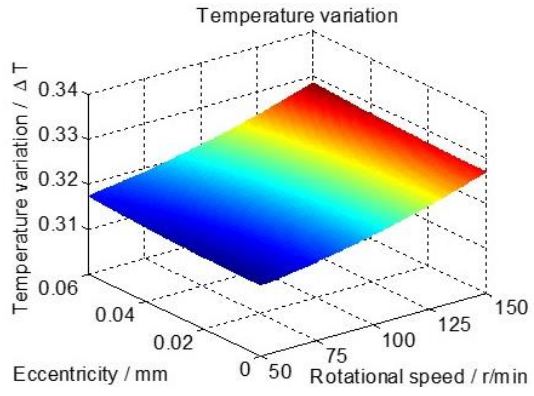

a

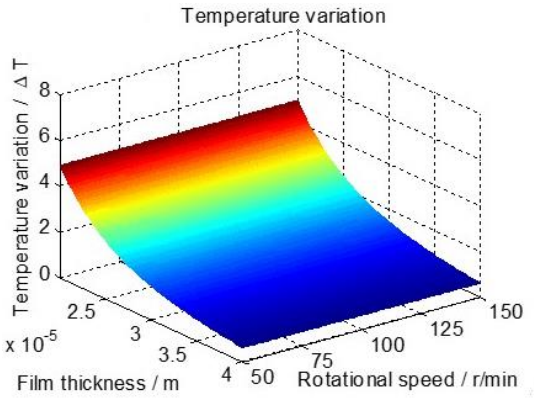

b

Fig. 4 The temperature variation of various conditions: a) eccentricity ratio; b) film thickness

thickness, which means the temperature variation is much close to the film thickness. It seems to be independent of the rotational speed increases from 50 to 150 r/min, which keeps consistent with that of Fig. 4, a.

Detailed data are listed in the following Tables 3 and 4. In Table 3, the temperature seems to be unchanged with the eccentricity ratio increases from 0.01 to 0.05. Detail data for temperature variation with 50 r/min are 0.315, 0.316, 0.316, 0.317 and 0.317°C, respectively. Not only that, a slight temperature variation is noticed with the rotational speed increases from 50 to 150 r/min. The temperature variation with an eccentricity ratio of 0.01 is 0.315, 0.317, 0.320, 0.323 and 0.327°C, respectively. That means the temperature variation is slightly affected by the eccentricity ratio and rotational speed.

Meanwhile, the results in Table 4 show the temperature variation with film thickness from 0.02 to 0.04 mm is much obvious. The temperature variation is 4.918, 2.519, 1.459, 0.919 and 0.616 °C with the film thickness ranges from 0.02 to 0.04 mm. It shows a rapid decrease with increasing film thickness, which means the temperature variation is much close with the film thickness. While the temperature variation is 4.918, 4.923, 4.928, 4.936 and 4.945 °C with the rotational speed ranges from 50 to 150 r/min. It seems to be independent of the rotational speed increases from 50 to 150 r/min, which keeps consistent with that of Table 3. It can be concluded from Tables 3 and 4 that the temperature variation is much more sensitive to the film thickness.

Table 3

Temperature variation with various rotational speed and eccentricity ratio.

ΔT °C	50 r/min	75 r/min	100 r/min	125 r/min	150 r/min
ε=0.01	0.315	0.317	0.320	0.323	0.327
ε=0.02	0.316	0.317	0.320	0.323	0.327
ε=0.03	0.316	0.318	0.320	0.323	0.327
ε=0.04	0.316	0.318	0.321	0.324	0.328
ε=0.05	0.317	0.319	0.321	0.324	0.328

Table 4

Temperature variation with various rotational speed and film thickness.

ΔT °C	50 r/min	75 r/min	100 r/min	125 r/min	150 r/min
h_0=0.020	4.918	4.923	4.928	4.936	4.945
h_0=0.025	2.519	2.523	2.523	2.533	2.541
h_0=0.030	1.459	1.461	1.465	1.470	1.477
h_0=0.035	0.919	0.922	0.925	0.929	0.937
h_0=0.040	0.616	0.618	0.621	0.625	0.630

In general, the temperature variation is more sensitive to the film thickness than that of the rotational speed and eccentricity ratio. It can be found that a larger temperature variation will be produced with a larger eccentricity ratio and rotational speed, and a smaller film thickness.

As it is noticed that the temperature variation of thermal conduction will be affected by above-mentioned impact factors. The influence of thermal conduction on the THD lubrication of the bearing will be discussed. Two specific cases with various film thicknesses and eccentricity ratios are defined over a range of rotational speed. The THD lubrication, including load capacity, bearing stiffness, friction power and flow power with variable temperature and constant temperature are thus compared to investigation the influence of thermal conduction.

5.1. Effect of film thickness on THD lubrication

As the results in Figs. 2 and 3 indicate that the load capacity and bearing stiffness is closely related to the eccentricity ratio. The results in Fig. 5 indicate the THD lubrication with various eccentricities ratio and rotational speeds. It is shown that the load capacity in Fig. 5, a increases with eccentricity ratio as a linear relationship and the bearing stiffness in Fig. 5, b seems to be a nonlinear increase with increasing eccentricity ratio, as predicted in Figs. 2, b and b.

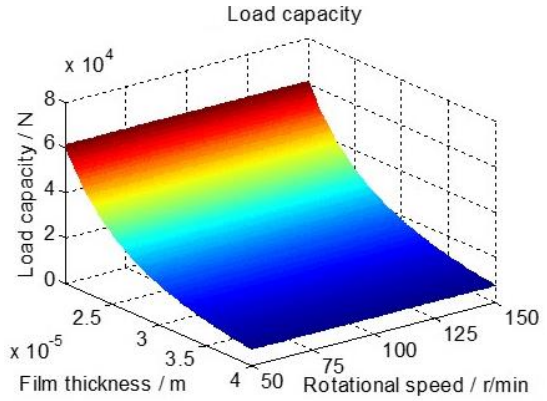

a

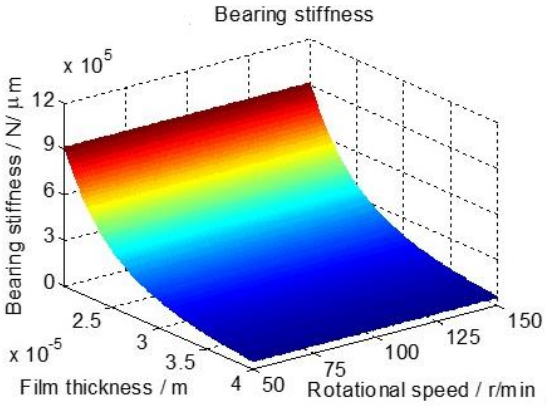

b

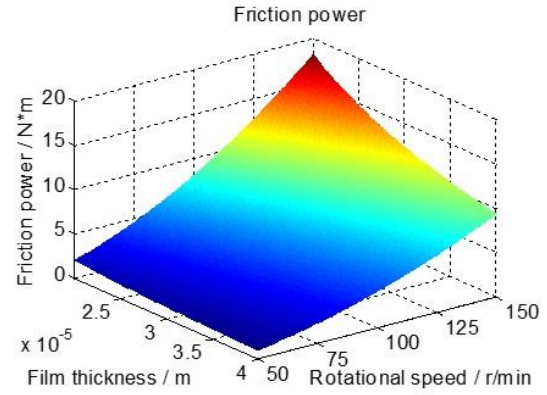

c

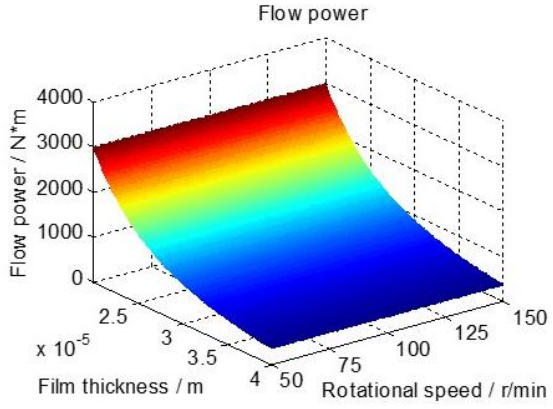

d

Fig. 5 The THD lubrication of various film thickness: a) load capacity; b) bearing stiffness; c) friction power; d) flow power

Both are found to be independent of the rotational speed. The friction power in Fig. 5, c indicates a close relationship with the rotational speed, as predicted in Eq. (14). And the flow power in Fig. 5, d is more related to the eccentricity ratio, while the variation is found to be much slight. The effect of friction power and flow power, it resulted in thermal conduction of the oil between the shaft and bearing.

5.2. Effect of eccentricity ratio

The results in Fig. 6 show the THD lubrication over a range of eccentricity and rotational speed. The Fig. 6, a shows that the load capacity decreases gradually with the film thickness and remains unchanged with increased rotational speed, which is noticed to be consistent with the results in Figs. 2, b and 3, b. A similar response can be noticed

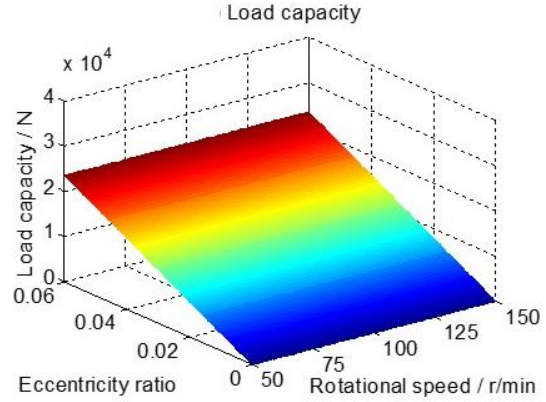

a

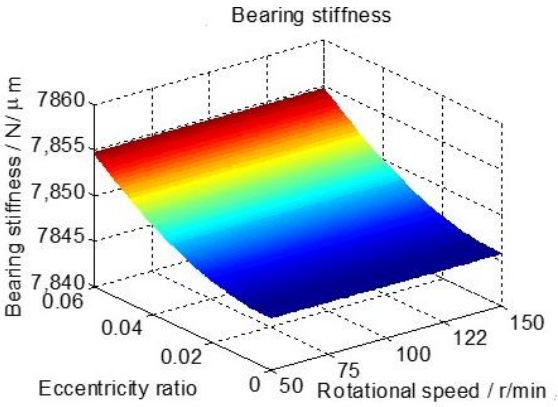

b

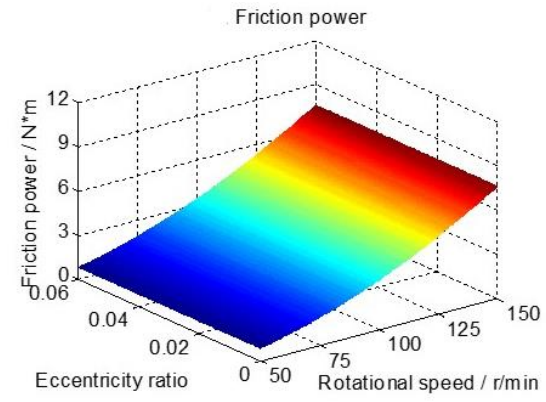

c

Fig. 6 The THD lubrication of various eccentricity ratio: a) load capacity; b) bearing stiffness; c) friction power; d) flow power

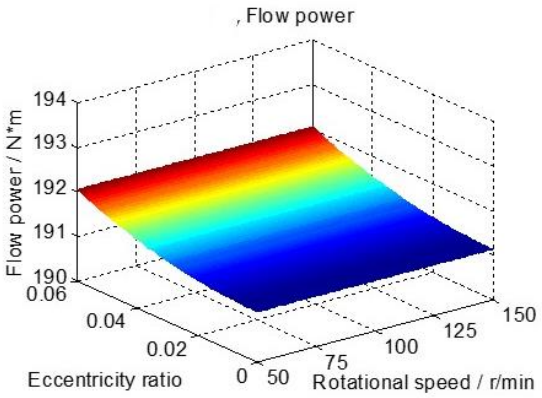

d

Fig. 6 Continuation

for the bearing stiffness in Fig. 6, b, which keeps good agreement with that of Figs. 2, c and 3, c. While the friction power in Fig. 6, c shows a slight increase with film thickness and a rapid enlargement as rotational speed increased. Both impact factors cause significant variations of friction power in nonlinearity. The flow power indicates a rapid decrease with increasing film thickness. And the variation is much larger than the effect of the eccentricity ratio in Fig. 6, d.

6. Comparison and discussion

In order to investigate the influence of thermal conduction on the lubrication behavior more clearly, a comparison of the results with constant temperature and variable temperature is thus conducted. As previous results indicate that the effect of eccentricity ratio and film thickness is more significant, which are thus selected as the conditional variables. The lubrication behavior, including load capacity and bearing stiffness is defined as the results of the comparison for simplification.

The results in Fig. 7 show the influence of thermal conduction on THD lubrication with the eccentricity ratio ranges from 0.01 to 0.05 and the film thickness in-creases from 0.02 to 0.04 mm, respectively. The comparison of load capacity with constant and variable temperature is shown in Fig. 7, a, and that of bearing stiffness is illustrated in Fig. 7, b. The result of constant temperature is noticed to be much larger than that of the variable temperature. The load capacity under constant temperature increases from 5.358 to 2.679 kN with the eccentricity ratio ranges from 0.01 to 0.05. And that of the variable temperature increases from 3.923 to 1.962 kN. The difference between both cases is noticed to be enlarged with increasing eccentricity ratio. The bearing stiffness seems to change slightly with the eccentricity ratio, while the difference for both kinds of working temperatures can be found to be much significant. That mean variable temperature can decrease the THD lubrication of the bearing, especially for the bearing stiffness with a larger eccentricity ratio.

As the variation of film thickness with the lower values is much more sensitive, the values of 0.02, 0.025, 0.03, 0.035 and 0.04 mm are selected for the comparison. The responses of load capacity with variable temperature are similar to those of constant temperature, shown in Fig. 8, a. From the specific data, the load capacity decreases from 87.06 to 10.88 kN for the constant temperature with increasing film thickness. And it is 61.27 to 7.67 kN for the case of variable temperature. The degree of decrease trends to be smaller with increasing film thickness for both cases. Without doubt, it can be concluded that variable temperature produces a significant decrease in the load capacity. Meanwhile, similar results can be found for the comparison between bearing stiffness, shown in Fig. 8, b. And the stiffness difference of constant and variable temperature seems to be more obvious.

In general, it can be noticed that variable temperature will decrease the load capacity and bearing stiffness.

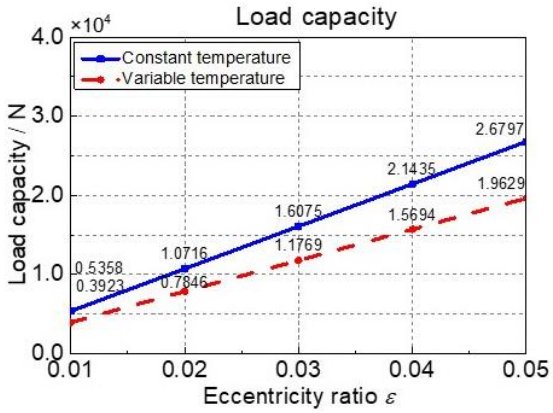

a

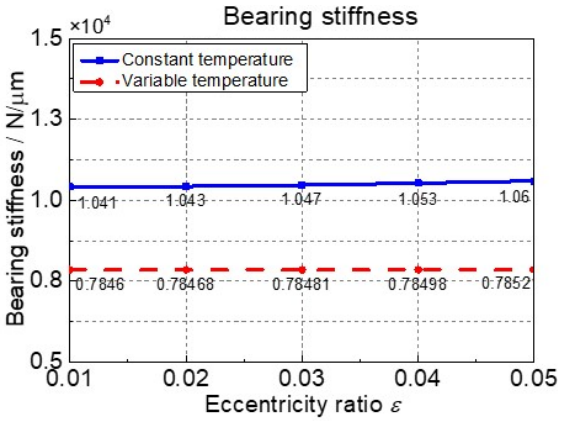

b

Fig. 7 The comparison of constant and variable temperature: a) load capacity; b) bearing stiffness

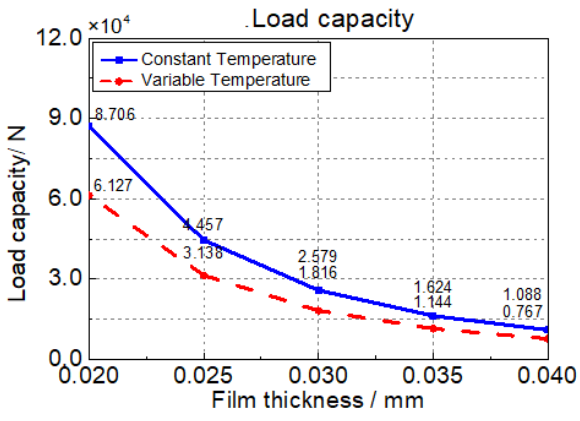

a

Fig. 8 The comparison of constant and variable temperature: a) load capacity; b) bearing stiffness

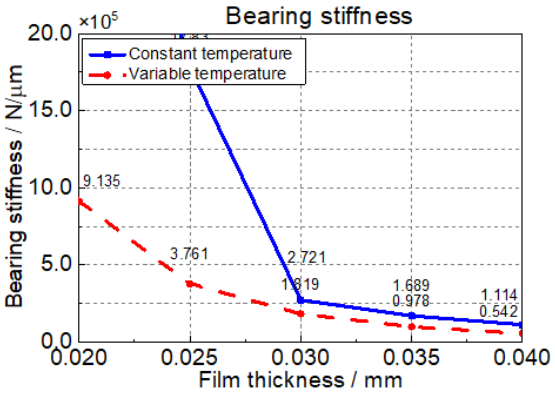

b

Fig. 8 Continuation

and the influence under the working condition of a larger eccentricity ratio and a smaller film thickness is more significant.

7. Conclusions

In summary, this paper provides a theoretical model regarding the lubrication behavior of hydrodynamic-static hybrid bearing with deep-shallow chambers considering thermal conduction. The fluid pressure, load capacity, bearing stiffness and flow rate are investigated with the centered finite difference method. The impact factors of film thickness, working temperature and eccentricity ratio are analyzed. Moreover, the temperature variation of thermal conduction is obtained. And the lubrication behavior with constant and variable temperature are compared to investigate the influence of thermal conduction. Three further contributions can be given:

First, the lubrication behavior includes fluid pressure, load capacity, bearing stiffness and flow rate is closely related to the film thickness, working temperature and eccentricity ratio.

Second, the temperature variation of thermal conduction is more significant with larger eccentricity ratio, higher rotational speed and smaller film thickness.

Finally, the friction power and flow power of THD lubrication is sensitive to temperature variation, which will cause decreases in the load capacity and bearing stiffness.

In order to increase the service life of the journal bearing, the interactions of temperature, pressure, viscosity and other impact factors will be considered in future work.

Acknowledgments

This research was funded by the National Natural Science Foundation of China (No. 52272377 & 51809201), the found of Key Laboratory of Marine Power Engineering & Technology (Wuhan University of Technology), Ministry of Transport (No. KLMPET2018-05).

References

1. **Du, Y.; Mao, K.; Chen, H.;** et al. 2018. Effect of fluid compressibility on the transient response characteristics of open-type constant flow hydrostatic bearings, Tribology Letters 66(0): 9. http://dx.doi.org/10.1007/s11249-017-0959-9.
2. **Zhai, L.; Luo, Y.; Liu, X.;** et al. 2017. Numerical simulations for the fluid-thermal-structural interaction lubrication in a tilting pad thrust bearing, Engineering Computations 34(4): 1149-1165. http://dx.doi.org/10.1108/EC-08-2015-0209.
3. **Ostayen, R.** 2010. Film height optimization of dynamically loaded hydrodynamic slider bearings, Tribology International 43(0): 1786-1793. http://dx.doi.org/10.1016/j.triboint.2010.04.009.
4. **Wang, L.; Han, Z.; Chen, G.;** et al. 2017. Thermo-hydrodynamic analysis of large-eccentricity hydrodynamic bearings with texture on journal surface, Proceedings of the Institution of Mechanical Engineers-Part C: Journal of Mechanical Engineering Science 203-210(0): 1-6. http://dx.doi.org/10.1177/0954406217739646.
5. **Litwin, W.** 2010. Influence of main design parameters of ship propeller shaft water-lubricated bearings on their properties, Polish Maritime Research 17(4): 39-45. http://dx.doi.org/10.2478/v10012-010-0034-z.
6. **Wodtke, M.; Schubert, A.; Fillon, M.;** et al. 2014. Large hydrodynamic thrust bearing: comparison of the calculations and measurements, Proceedings of the Institution of Mechanical Engineers, Part J: Journal of Engineering Tribology 228(9): 974-983. http://dx.doi.org/10.1177/1350650114528317.
7. **Dąbrowski, L.; Pajączkowski, P.; Rotta, G.;** et al. 2013. Improving performance of large thrust bearings through modeling and experimentation, Mechanics & Industry 14(4): 267-274. http://dx.doi.org/10.1051/meca/2013064.
8. **Lu, D.; Liu, K.; Zhao, W.;** et al. 2016. Thermal characteristics of water-lubricated ceramic hydrostatic hydrodynamic hybrid bearings, Tribology Letters 63(0): 23. http://dx.doi.org/10.1007/s11249-016-0711-x.
9. **Wodtke, M.; Fillon, M.; Schubert, A.;** et al. 2013. Study of the influence of heat convection coefficient on predicted performance of a large tilting-pad thrust bearing, Journal of Tribology-Transactions of the ASME 132(5): 021702. http://dx.doi.org/10.1115/1.4023086.
10. **Dang, P.; Chatterton, S.; Pennacchi, P.;** et al. 2018. Numerical investigation of the effect of manufacturing errors in pads on the behaviour of tilting-pad journal bearings, Proceedings of the Institution of Mechanical Engineers, Part J: Journal of Engineering Tribology 232(4): 480-500. http://dx.doi.org/10.1177/1350650117721118.
11. **Laraqi, N.; Rashidi, M.; J. G. d. Maria;** et al. 2011. Analytical model for the thermo-hydrodynamic behaviour of a thin lubricant film. Tribology International 44(0): 1083-1086. http://dx.doi.org/10.1016/j.triboint.2011.04.012.
12. **Boubendir, S.; Larbi, S.; Bennacer, R.** 2011. Numerical study of the thermo-hydrodynamic lubrication phenomena in porous journal bearings., Tribology International 44(0): 1-8. http://dx.doi.org/10.1016/j.triboint.2010.09.008.
13. **Armentrout, R.; He, M.; Haykin, T.;** et al. 2017. Analysis of turbulence and convective inertia in a water-lubricated tilting-pad journal bearing using conventional and CFD approaches, Tribology Transactions 60(6): 1129-1147. http://dx.doi.org/10.1080/10402004.2016.1251668.

14. **Singh, U.; Roya, L.; Sahu, M.** 2008. Steady-state thermo-hydrodynamic analysis of cylindrical fluid film journal bearing with an axial groove, Tribology International 41(0): 1135-1144. http://dx.doi.org/10.1016/j.triboint.2008.02.009.
15. **Roy, L.** 2009. Thermo-hydrodynamic performance of grooved oil journal bearing, Tribology International 44(0): 1187-1198. http://dx.doi.org/10.1016/j.triboint.2009.04.001.
16. **Zhang, X.; Yin, Z.; Jiang, D.;** et al. 2014. The design of hydrodynamic water-lubricated step thrust bearings using CFD method, Mechanics & Industry 15(3): 197-206. http://dx.doi.org/10.1051/meca/2014026.
17. **Wang, Y.; Shi, X.; Zhang, L.;** 2014. Experimental and numerical study on water-lubricated rubber bearings, Industrial Lubrication and Tribology 66(2): 282-288. http://dx.doi.org/10.1108/ILT-11-2011-0098.
18. **Zhang, Y.; Sun, J.; Kong, P.;** et al. 2019. Research on the oil film temperature field of hydrostatic bearing with variable viscosity dynamic simulation and experiment, Proceedings of the Institution of Mechanical Engineers, Part J: Journal of Engineering Tribology 233(11): 1763-1772. http://dx.doi.org/10.1177/1350650119846002.
19. **Jiang, X.; Wang, J.; Fang, J.** 2011. Thermal elastohydrodynamic lubrication analysis of tilting pad thrust bearings, Proceedings of the Institution of Mechanical Engineers, Part J: Journal of Engineering Tribology 25(J2): 51-57. http://dx.doi.org/10.1177/2041305X10394408.
20. **Yang, J.; Palazzolo, A.** 2019. Three-dimensional thermo-elasto-hydrodynamic computational fluid dynamics model of a tilting pad journal bearing-Part II: dynamic response, Journal of Tribology 141(6): 061703. http://dx.doi.org/10.1115/1.4043350.
21. **Suh, J.; Palazzolo, A.** 2015. Three-dimensional dynamic model of TEHD tilting-pad Journal bearing-Part I: theoretical modeling, Journal of Tribology-Transactions of the ASME 137(4): 041703. http://dx.doi.org/10.1115/1.4030020.
22. **Lin, Q.; Wei, Z.; Wang, N.;** et al. 2013. Analysis on the lubrication performances of journal bearing system using computational fluid dynamics and fluid-structure interaction considering thermal influence and cavitation, Tribology International 64(0): 8-15. http://dx.doi.org/10.1016/j.triboint.2013.03.001.
23. **Du, Y.; Li, M.** 2020. Effects on lubrication characteristics of water-lubricated rubber bearings with journal tilting and surface roughness, Proceedings of the Institution of Mechanical Engineers, Part J: Journal of Engineering Tribology 234(2): 161-171. http://dx.doi.org/10.1177/1350650119858573.
24. **Dang, P.; Chatterton, S.; Pennacchi, P.;** et al. 2016. Effect of the load direction on non-nominal five pad tilting-pad journal bearings, Tribiology International 98(0): 197-211 . http://dx.doi.org/10.1016/j.triboint.2016.02.028.
25. **Liang, X.; Yan, X.; Ouyang, W.;** et al. 2019. Thermo-Elasto-Hydrodynamic analysis and optimization of rubber supported water-lubricated thrust bearings with polymer coated pads, Tribology International 138(0): 365-379. http://dx.doi.org/10.1016/j.triboint.2019.06.012.
26. Substech. http://www.substech.com/dokuwiki/doku.php?id=hydrodynamic_journal_bearing.
27. **Wen, S.** 1991. Tribology theory. Beijing: Publishing Company of Tsinghua University.
28. **Chen, Y.** 1980. Principle and design of hydrostatic support. Beijing: National Defense Industry Press.
29. **Meng, S.; Xiong, W.; Wang, S.;** et al. 2015. Analytical research on characteristics of deep-shallow journal bearings with orifice restrictors, Journal of Mechanical Engineering 51(22): 191-201. http://dx.doi.org/10.3901/JME.2015.22.191.

Q. Huang, Z. Zhao, H. Liu

LUBRICATION ANALYSIS OF HYDRODYNAMIC-STATIC HYBRID BEARING WITH DEEP-SHALLOW CHAMBERS CONSIDERING THERMAL CONDUCTION

S u m m a r y

The oil film separates the shaft-bearing system to reduce the frictional force of contact surfaces with large temperature variations owing to thermal conduction. Multiple impact factors seriously affected the lubrication behavior of the bearing during actual working process. An applicable model regarding the lubrication analysis of a hydrodynamic-static hybrid bearing with deep-shallow chambers is proposed and validated with published literature. The lubrication behavior includes film pressure, load capacity, bearing stiffness and flow rate is numerically calculated with centered finite difference method by solving the Reynolds equation. The influence of film thickness and working temperature are considered, over a range of eccentricity ratio. Moreover, the temperature variation caused by thermal conduction is analyzed in details. To investigate the influence of thermal conduction on the lubrication behavior, the results show that the load capacity, bearing stiffness, friction power, and flow power significantly decline with the consideration of thermal conduction. This study proposes an accurate model that is helpful for the design of hydrodynamic-static hybrid bearings with deep-shallow chambers under low rotational speed, heavy load, and high temperature conditions.

Keywords: lubrication analysis, thermal conduction, temperature variation, hydrodynamic-static hybrid bearing, deep-shallow chambers

Received January 12, 2023
Accepted August 2, 2023